

Reclaimed Asphalt Test Specimen Preparation Assisted by Image Analysis

D. Lo Presti¹; N. A. Hassan²; R. Khan³; and G. Airey⁴

Abstract: This paper presents a laboratory investigation aimed at establishing a protocol for the production of homogeneous asphalt mixtures test specimens, incorporating reclaimed asphalt by using a gyratory compactor with coring and trimming works. Stone mastic asphalt specimens were compacted at the previously identified target densities with the final aim of obtaining specimens with a fixed and homogeneous air void distribution. A microstructural study was conducted to characterize the homogeneity in the air void distribution using X-ray computed tomography (CT) combined with image analysis techniques. The study concluded that the gyratory compactor is suitable for producing homogeneous test specimens for the specified mixtures and a set of detailed procedures has been proposed for the production of the compacted specimens and to perform the microstructural study. DOI: 10.1061/(ASCE)MT.1943-5533.0001012. This work is made available under the terms of the Creative Commons Attribution 4.0 International license, <http://creativecommons.org/licenses/by/4.0/>.

Author keywords: X-ray computed tomography (CT); Image analysis; Gyratory compactor; Reclaimed asphalt; Re-Road.

Introduction

For a decade, the application of imaging technology in the microstructure study of asphalt mixtures has become significant. A number of studies have used the advanced technology of X-ray computed tomography (CT) combined with image analysis techniques in asphalt mixtures due to its ability to nondestructively characterize the internal structure properties such as the air void distribution, aggregates structure and damage (Masad et al. 1999a; Tashman et al. 2001; Masad et al. 2002; Khan 2009; Kutay et al. 2010; Hassan et al. 2012). Currently, a few studies have used this imaging technique to evaluate the compaction homogeneity for laboratory-fabricated specimens in order to produce a homogeneous gyratory compacted specimen (Muraya 2007; Tashman et al. 2007). The superpave gyratory compactor allows preparing asphalt samples by simulating actual field compaction. Such compaction is achieved by combining a rotary shearing action and a vertical resultant force applied by a mechanical head. This helps in achieving specimens of given dimensions at a predetermined density for subsequent testing of their mechanical properties.

For laboratory testing, the asphalt mixture specimen is assumed to be homogeneous when the specimen has the same material proportions, including air voids throughout its volume, to create a consistent mixture. However, previous studies on the gyratory

compacted specimens have reported that higher air voids were observed at the top and bottom than at the middle section of the specimen, indicating the nonhomogeneity in the laboratory compaction (Masad et al. 1999b, 2002). In addition, studies by Tashman et al. (2004) and Thyagarajan et al. (2009) found that the specimen height and diameter play a significant role in the variability of the compaction energy and the air void distribution as well as variation in density. This has raised an issue of the importance of establishing a method of compaction in order to produce a homogeneous test specimen to get a reliable test result that will lead to an appropriate evaluation of the materials' mechanical properties. Therefore, this study has used X-ray CT scanning and common laboratory techniques to establish a protocol for manufacturing a homogenous gyratory compacted specimen for laboratory testing.

Material and Methods

In this study, three types of stone mastic asphalt (SMA11S) mixtures were selected: a virgin mixture (V-mix) and two mixtures added with 15 and 30% of reclaimed asphalt (RA-mix). All mixtures were designed with similar grading curve (Fig. 1) and blended with polymer-modified binder. Mixes and binder properties are summarized in Table 1. All mixtures were designed with a similar grading curve (Fig. 1) and by using binders with similar physical properties (PmB 25/55-55A). The binders have been recovered from the mixes [BS EN 13074-2, British Standards Institution (BSI) (2011)] and further characterized.

The gyratory compacted specimens were prepared in accordance with BS EN 12697-31:2007 (BSI 2007c) to achieve the reference density, which is equivalent to a 2.6% air void content that was obtained using a previous Marshall mix design procedure (Table 1). In order to establish an optimized procedure, the effect of height/diameter ratio (H/D) has been investigated (1.0 and 1.5) by compacting specimens with different combinations of height and diameter (100 and 150 mm). The compaction was conducted at 145°C ($\pm 5^\circ\text{C}$) with a vertical pressure of 600 kPa, internal angle, 0.82° and the speed of rotation of 30 gyrations/min.

¹Univ. of Nottingham, Pavement Research Building, University Park, NG7 2RD, U.K. (corresponding author). E-mail: davide.lopresti@nottingham.ac.uk

²Universiti Teknologi Malaysia, Faculty of Civil Engineering and Transportation Research Alliance, Skudai 81310, Johor, Malaysia. E-mail: hnorhidayah@utm.my

³Univ. of Engineering and Technology, Peshawar, Faculty of Civil Engineering, University Campus, Peshawar, Pakistan. E-mail: rawid806@gmail.com

⁴Univ. of Nottingham, Pavement Research Building, University Park, NG7 2RD, U.K. E-mail: gordon.airey@nottingham.ac.uk

Note. This manuscript was submitted on August 30, 2013; approved on December 27, 2013; published online on January 2, 2014. Discussion period open until December 8, 2014; separate discussions must be submitted for individual papers. This paper is part of the *Journal of Materials in Civil Engineering*, © ASCE, ISSN 0899-1561/C4014005(5)/\$25.00.

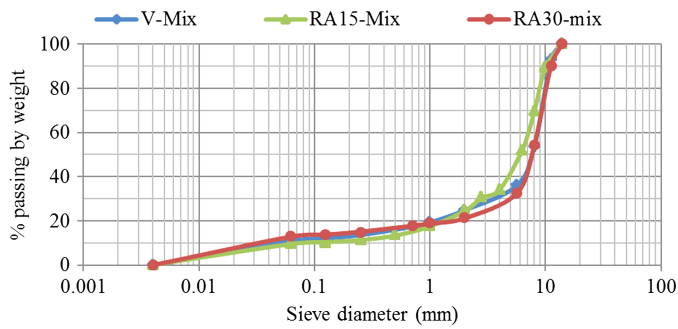


Fig. 1. Aggregate grading curves of V-mix and RA-mixes

Table 1. Properties of V-mix and RA-mix

Properties	Mix type		
	V-mix		RA mixes
	SMA 11S (0% RA)	SMA 11S (15% RA)	SMA 11S (30% RA)
Maximum density (kg/m ³)	2,454	2,494	2,485
Binder content (%)	6.5	5.6	7.2
[BS EN 13074-2 (BSI 2011)]			
Binder pen [BS EN 1426 (BSI 2007a)] (dmm)	30	32	21
Binder SP [BS EN 1427 (BSI 2007b)] (°C)	64.2	64.2	70.8
Viscosity @150°C [BS EN 13302 (BSI 2010)] (Pa.s)	0.63	0.64	1.06

X-Ray CT and Image Analysis

A Venlo H-350/225 X-ray CT system (shaw inspection systems) with the *IMPS* operating software was used for capturing the two-dimensional (2D) images at the interval of 1 mm along the specimen height with a resolution of approximately 0.083 mm/pixel (Figs. 2 and 3). The imaging software, *ImageJ*, was used to threshold the air void particles from X-ray images and the volume fraction was calculated using Eq. (1). The result was then validated through comparison with the one measured using the buoyancy test method. The thresholded images of the air voids were then analyzed for specimen's homogeneity assessment.

$$\text{Area fraction} = \frac{\text{Air voids area(mm}^2\text{)}}{\text{Total image area(mm}^2\text{)}} \times 100 \quad (1)$$

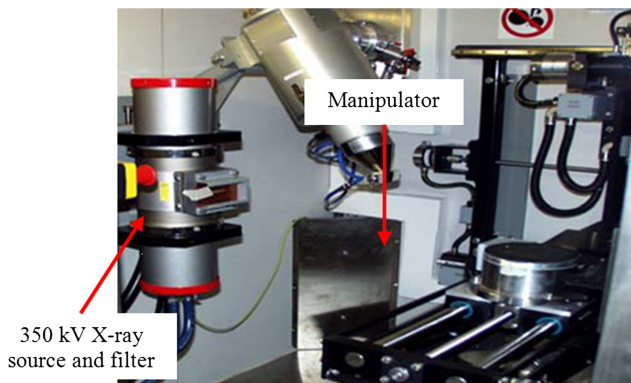


Fig. 2. X-ray CT equipment

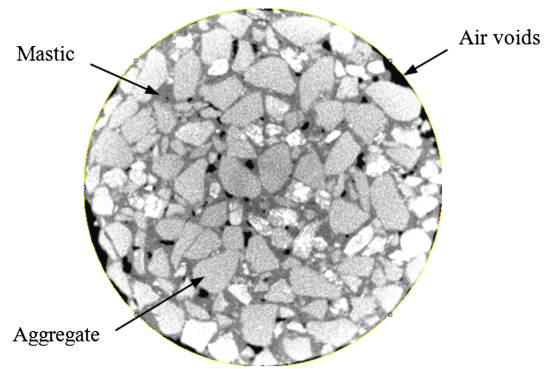


Fig. 3. 2D X-ray CT image of the specimen

At first, the homogeneity of the air void distribution was assessed using cores and ring analysis. In this analysis, the images were virtually cut into cores of increasing radius (25 mm) from the center of the specimen to the specimen's edge and the rings of increasing radius (25 mm) from the edge to the center of the specimen. The air void distribution within the cores and rings were then analyzed. Subsequently, another analysis was conducted to quantify the uniformity of the air void distribution across the depth of the specimen in vertical and radial directions [Eqs. (2) and (3)]. The latter applies the concept of uniformity index (UI) introduced by Masad et al. (2009). For UI vertical the polynomial function, $f(x)$ is a function of air void percentage, x over the specimen height limits a and b . The fourth-order polynomial of the function $f(x)$ is obtained from a best fitting of the plot of the measured air voids versus specimen height. For UI radial the polynomial function, $f(r)$ is calculated based on a function of air voids over the radius, r . A UI value close to zero indicates a uniform air void distribution.

$$\text{UI vertical} = \frac{1}{b-a} \int_a^b [f'(x)]^2 dx \quad (2)$$

$$\text{UI radial} = \frac{1}{R-0} \int_0^R [f'(r)]^2 dr \quad (3)$$

Manufacturing Homogenous Gyratory Specimen

Under this investigation, a set of procedures consisting of three methods of gyratory compaction have been conducted for obtaining a targeted test specimen of 100 × 100 mm with homogeneous air void distribution. On the assumptions that eventual difficulties in the compaction are proportional to the amount of RA, only the V-mix and RA30-mix have been considered. The methods are summarized as follows:

- Procedure A: Directly compacting 100 × 100 mm specimen (H/D:100/100);
- Procedure B: Trimming a 100 × 100 mm specimen from 150 × 100 mm specimen (H/D:150/100-slender specimen); and
- Procedure C: Coring and trimming the 100 × 100 mm specimen from 150 × 150 mm specimen (H/D:150/150).

Details of the compaction procedures B and C are illustrated in Fig. 4. The specimens were then X rayed for internal structure images and laboratory tested for air void content [Buoyancy test BS EN 12697-6:2012 (BSI 2012)]. Table 2 summarizes the specimen properties as a result of undertaking the three compaction procedures.

From Fig. 5, both virgin and RA specimens prepared with procedure A have higher air void content at the top and bottom sections compared with the middle section indicating nonuniformity in the

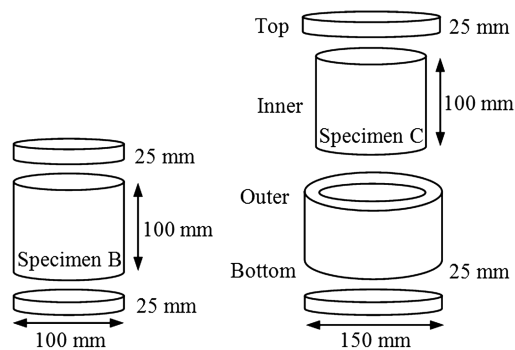


Fig. 4. Trimmings to obtain 100/100 cores from procedures B and C

Table 2. Specimen Properties from Procedures A, B, and C

Type	Specimen size (mm) (height/diameter)	GYRO air voids (%)	Buoyancy test air voids (%)	Vertical UI	Radial UI
Procedure A					
V-mix	100/100	2.49	2.95	1.182	0.033
RA30-mix	100/100	2.80	3.83	1.307	0.030
Procedure B					
V-mix	150/100	2.83	3.00	1.955	0.009
	Core 100/100	—	3.90	1.285	0.011
RA30-mix	150/100	2.78	3.27	0.006	0.008
	Core 100/100	—	4.65	0.026	0.010
Procedure C					
V-mix	150/150	2.83	1.83	0.0140	0.027
	Core 100/100	—	0.2	0.0003	0.0006
RA30-mix	150/150	2.82	2.00	0.0178	0.005
	Core 100/100	—	0.7	0.0008	0.001

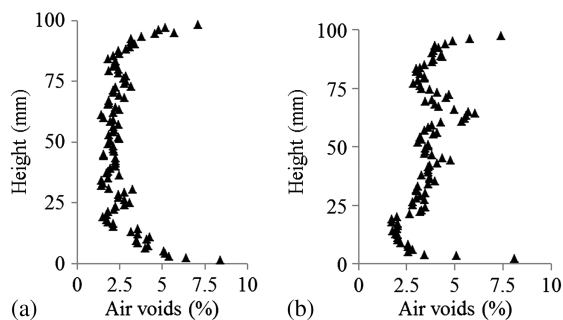


Fig. 5. Specimen A: air void distribution for (a) V-mix; (b) RA30-mix

air void distribution throughout the specimens. This agrees with the higher values obtained for the vertical uniformity index compared with the radial one. In fact, final trimming (at least 15 mm) is needed at both ends of the specimens due to uneven surfaces caused by the preset angle (0.82°) during compaction. As a result, procedure A allows obtaining a homogenous specimen but with an H/D ratio much lower than 1, which is not what was targeted. On the other hand, as presented in Fig. 6, the RA30 specimen, produced with H/D ratio higher than 1, shows more air voids at the middle of the specimen compared with the other sections. This shows that the slender specimen contains nonhomogenous air void distribution. However, when the specimen was produced using procedure C, in which the core of $D = 100$ mm was cored from a specimen with the original size of $D = 150$ mm, a homogenous air void distribution can be observed throughout the specimen

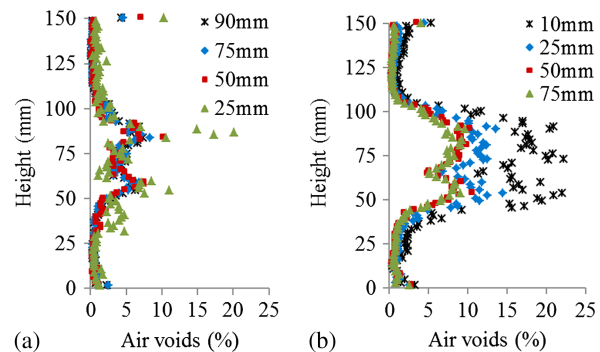


Fig. 6. Specimen B: inner cores (a) and outer rings; (b) analyses of compacted RA30-mix specimen

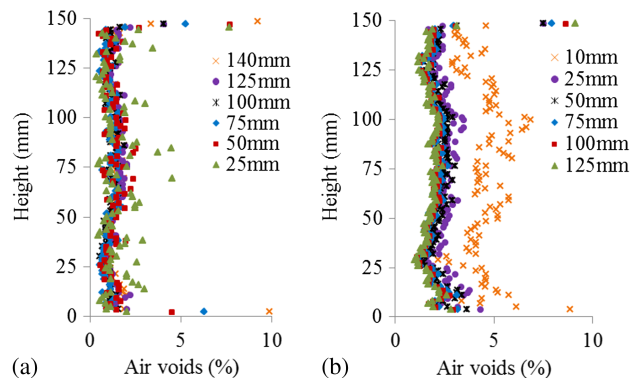


Fig. 7. Specimen C: inner cores (a) and outer rings; (b) analyses of compacted RA30-mix specimen

as shown in Fig. 7. It should be noted that high air void content observed on the first few slices on the top and bottom sections is caused by the cutting and trimming works.

Gyratory Compactor Settings to Achieve the Target Density

The second investigation of this study was to obtain a 100×100 mm specimen with homogenous air void distribution at the designed air void content. Using the compaction method proposed in procedure C, a preliminary investigation was carried out by compacting a number of 150×150 mm specimens at different densities for optimization (100, 95 and 90% from the original target density at 2.6% target air void content). Three replicates were prepared for each target density.

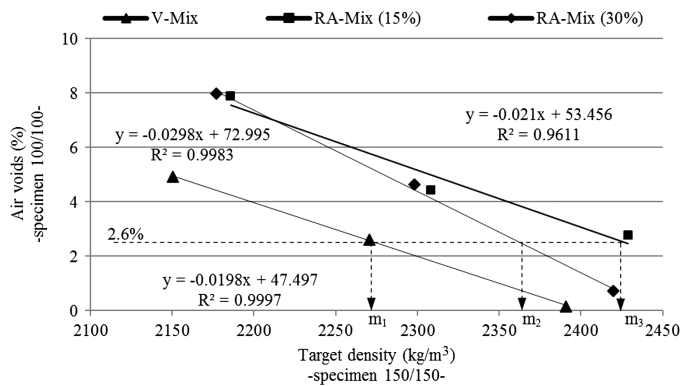
Table 3 summarizes the average values of resulting densities and air void contents of specimen C before and after the coring work. The idea was to obtain a relationship between the measured air void content of the cores (100×100 mm), and the target density to be set on the gyratory compactor for manufacturing the 150×150 mm specimens. The target density for compacting 150×150 mm specimen to obtain a core (100×100 mm) with homogenous air void content of 2.6% was then estimated from the linear relationships in Fig. 8 with the R -squared (R^2) values close to 1.

From the plot, the estimated target densities for all mixture types are as follows:

- V-mix: $m^1 = 2,267 \text{ kg/m}^3$, (95% of the original target);
- RA15-mix: $m^2 = 2,422 \text{ kg/m}^3$, (100% of the original target); and
- RA30-mix: $m^3 = 2,355 \text{ kg/m}^3$, (97% of the original target).

Table 3. Details Density and Air Voids for Optimization

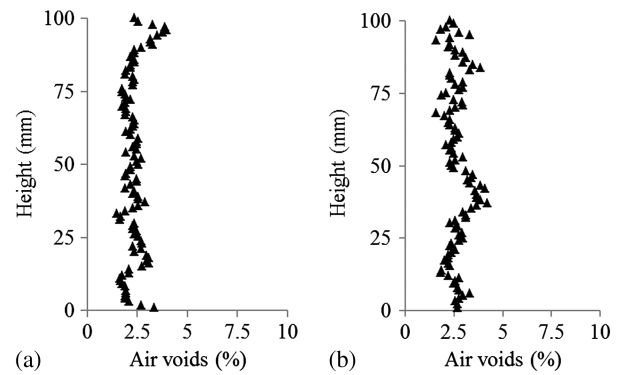
Type	Maximum density (kg/m ³)	Gyratory compacted specimen (150/150)		After coring (laboratory determined density of 100/100)
		Target density (kg/m ³)	Target air voids (%)	Average air voids (%)
V-mix	100%	2,391	2.6	0.15
	95%	2,271	7.5	2.6
	90%	2,151	12.3	4.9
RA15-mix	100%	2,429	2.6	2.75
	95%	2,308	7.5	4.4
	90%	2,186	12.3	7.85
RA30-mix	100%	2,420	2.6	0.7
	95%	2,298	7.5	4.6
	90%	2,177	12.4	7.95

**Fig. 8.** Relationships of the target air void content for 100/100 specimen and the density to be set during compaction for 150/150 specimen

In order to ensure repeatability of the test results, 24 replicates for each mixture type were then prepared by using the estimated density values. The cores of 100 × 100 mm were tested for air void content and X rayed for image analysis. This was to confirm that the specimens meet the target air void content (2.6%) and the air voids were homogeneously distributed through the 100 × 100 mm core. Table 4 and Fig. 9 give the results of the buoyancy test and an image analysis of the air void distribution. Both results prove that the cores of 100 × 100 mm (for all mixture types) with homogeneous air void distribution at the target air void content can be achieved using the method established in procedure C. Fig. 9 shows that the air void distributions in virgin and reclaimed asphalt specimens are uniformly distributed from top to bottom with average values differing around +0.5% from the desired one. The small variation in the average values indicates good repeatability within the replicates. This is also agreed by the uniformity index values calculated in both vertical and radial directions with the values close to zero (Table 4). In addition, the virgin mix shows

Table 4. Specimen (100/100) Properties after Optimization

Type	Buoyancy test		Image analysis	
	Density (kg/m ³)	Air voids (%)	Vertical UI	Radial UI
V-mix	2,380.17	3.01	0.012	0.019
RA15-mix	2,437.42	2.26	0.010	0.015
RA30-mix	2,433.33	2.08	0.002	0.152

**Fig. 9.** Specimen C (100 × 100 mm core): air void distribution for (a) V-mix; (b) RA30-mix

slightly less homogeneous air void distribution throughout the specimen than the RA-mix. This could be due to the downsizing process of the RA recovered from the asphalt pavement. In fact, fractionation of the reclaimed asphalt pavement involves crushing and screening, which can result in a reduction of the original size and shape of the aggregate particles (become rounded and uniform), this consequently affects the aggregate interlock in filling up the volume of the specimen during compaction.

Conclusion

From this study, the following conclusions can be drawn:

- X-ray CT scanning together with the proposed cores and rings analysis proved to be very useful tools to nondestructively assess the homogeneity of gyratory compacted asphalt specimens, even with the addition of an increasing percentage of reclaimed asphalt.
- Results of the image analyses proved that the dimension of the gyratory compacted specimen provides a significant effect on the air void distribution. In fact, compacting slender gyratory specimen with an H/D ratio of 1.5 involves a completely different compaction mechanism than that registered with an H/D ratio of 1.0. In fact, in the former, the air void's distribution shows an opposite trend with higher values in the core and lower values at the top and bottom. This makes this procedure inconvenient for producing homogeneous test specimens.
- A homogenous test specimen at the desired air void content can be achieved by performing an optimization study aiming at producing specimens with at least three densities ranging from 90 to 100% of the original target density plus further buoyancy density tests. This will lead to a good estimation of the target density to be set on the gyratory compactor. The incorporation of up to 30% of reclaimed asphalt does not imply any limitations to this procedure

Acknowledgments

This study has been developed within *Re-Road* a collaborative project financed under the 7th Framework Programme of the European Commission. The authors wish to acknowledge the support of the University of Nottingham, United Kingdom, and special thanks go to numerous laboratory personnel from Nottingham Transportation Engineering Centre who assisted in this study.

References

- British Standards Institution (BSI). (2007a). "Bitumen and bituminous binders. Determination of needle penetration." *BS EN 1426*, London.
- British Standards Institution (BSI). (2007b). "Bitumen and bituminous binders. Determination of the softening point. Ring and Ball method." *BS EN 1427*, London.
- British Standards Institution (BSI). (2007c). "Bituminous mixtures. Test methods for hot mix asphalt Specimen preparation by gyratory compactor." *BS EN 12697-31*, London.
- British Standards Institution (BSI). (2010). "Bitumen and bituminous binders. Determination of dynamic viscosity of bituminous binder using a rotating spindle apparatus." *BS EN 13302*, London.
- British Standards Institution (BSI). (2011). "Bitumen and bituminous binders. Recovery of binder from bituminous emulsion or cut-back or fluxed bituminous binders: Stabilisation after recovery by evaporation." *BS EN 13074-2*, London.
- British Standards Institution (BSI). (2012). "Bituminous mixtures. Test methods for hot mix asphalt: Determination of bulk density of bituminous specimens." *BS EN 12697-6*, London.
- Hassan, N. A., Airey, G. D., Khan, R., and Collop, A. C. (2012). "Non-destructive characterization of the effect of asphalt mixture compaction on aggregate orientation and segregation using x-ray computed tomography." *Int. J. Pavement Res. Technol.*, 5(2), 84–92.
- ImageJ* [Computer software]. Bethesda, MD, National Institutes of Health.
- Khan, R. (2009). "Quantification of microstructural damage in asphalt." Ph.D. thesis, Univ. of Nottingham, Nottingham, U.K.
- Kutay, M. E., Arambula, E., Gibson, N., and Youtcheff, J. (2010). "Three-dimensional image processing methods to identify and characterise aggregates in compacted asphalt mixtures." *Int. J. Pavement Eng.*, 11(6), 511–528.
- Masad, E., Jandhyala, V., Dasgupta, N., Somadevan, N., and Shashidhar, N. (2002). "Characterization of air void distribution in asphalt mixes using x-ray computed tomography." *J. Mater. Civ. Eng.*, 10.1061/(ASCE)0899-1561(2002)14:2(122), 122–129.
- Masad, E., Kassem, E., and Chowdhury, A. (2009). "Application of imaging technology to improve the laboratory and field compaction of HMA." *Rep. No. FHWA/TX-09/0-5261-1*, Texas Transportation Institute, Texas A&M Univ., College Station, TX.
- Masad, E., Muhunthan, B., Shashidhar, N., and Harman, T. (1999a). "Effect of compaction procedure on the aggregate structure in asphalt concrete." *Transportation Research Record 1681*, Transportation Research Board, Washington, DC, 179–185.
- Masad, E., Muhunthan, B., Shashidhar, N., and Harman, T. (1999b). "Internal structure characterization of asphalt concrete using image analysis." *J. Comput. Civ. Eng.*, 10.1061/(ASCE)0887-3801(1999)13:2(88), 88–95.
- Muraya, P. M. (2007). "Homogeneous test specimens from gyratory compaction." *Int. J. Pavement Eng.*, 8(3), 225–235.
- Tashman, L., Masad, E., Little, D., and Lytton, R. (2004). "Damage evolution in triaxial compression tests of HMA at high temperatures." *J. Assoc. Asphalt Paving Technol.*, 73, 53–81.
- Tashman, L., Masad, E., Peterson, B., and Saleh, H. (2001). "Internal structure analysis of asphalt mixes to improve the simulation of superpave gyratory compaction to field conditions." *J. Assoc. Asphalt Paving Technol.*, 70, 605–645.
- Tashman, L., Wang, L. B., and Thyagarajan, S. (2007). "Microstructure characterisation for modelling HMA behaviour using imaging technology." *Int. J. of Road Mater. Pavement Des.*, 8(2), 207–238.
- Thyagarajan, S., Tashman, L., Masad, E., and Bayomy, F. (2010). "The heterogeneity and mechanical response of hot mix asphalt laboratory specimens." *Int. J. Pavement Eng.*, 11(2), 107–121.